Gutzwiller Monte Carlo approach for a critical dissipative spin model

Wim Casteels,[1] Ryan M. Wilson,[2] and Michiel Wouters[1]

[1]*TQC, Universiteit Antwerpen, Universiteitsplein 1, B-2610 Antwerpen, Belgium*
[2]*Department of Physics, The United States Naval Academy, Annapolis, Maryland 21402, USA*

We use the Gutzwiller Monte Carlo approach to simulate the dissipative XYZ model in the vicinity of a dissipative phase transition. This approach captures classical spatial correlations together with the full on-site quantum behavior while neglecting nonlocal quantum effects. By considering finite two-dimensional lattices of various sizes, we identify a ferromagnetic and two paramagnetic phases, in agreement with earlier studies. The greatly reduced numerical complexity of the Gutzwiller Monte Carlo approach facilitates efficient simulation of relatively large lattice sizes. The inclusion of the spatial correlations allows to capture parts of the phase diagram that are completely missed by the widely applied Gutzwiller decoupling of the density matrix.

I. INTRODUCTION

In recent years there has been a growing interest in the quantum behavior of dissipative systems (see, for example, the reviews [1–3]), which can be realized with various experimental platforms including ultracold atoms, trapped ions, superconducting circuits, semiconductor microcavities, and microwave cavities. Correspondingly, there is a renewed interest in dissipative phase transitions and critical behavior in these systems [4–11], which were recently observed experimentally [12–16]. The numerical description of these critical phenomena is notoriously difficult due to various factors including the exponentially large Hilbert space, the large entropy, and the critical slowing down of the dynamics. This has motivated various theoretical efforts towards the development of efficient simulation techniques for dissipative systems (see, for example, Refs. [17–26]).

The dissipative XYZ model is a spin model on a lattice described by the anisotropic XYZ-Heisenberg Hamiltonian and a spontaneous decay along the z direction. A very rich mean-field (MF) phase diagram was predicted for this system in Ref. [27]. In Ref. [28], short-range correlations were included in the description, which changed the topology of the phase diagram—a remarkable feature not observed for a system at equilibrium. In particular, they identified and examined a ferromagnetic to paramagnetic phase transition, which was not captured by the mean-field approach of Ref. [27]. More recently, the susceptibility, the entropy, and the Fisher information were examined with the corner-space renormalization method for two-dimensional (2D) lattices with a system size of up to 6×6 sites [29]. Possible experimental realizations of the dissipative XYZ model with trapped ions or ultracold atoms are discussed in Ref. [27]. Therein, they show that the model parameters can be externally tuned, which in principle can provide experimental access to interesting regions of the phase diagram.

In this paper, we apply the Gutzwiller Monte Carlo approach to the dissipative XYZ model to examine the ferromagnetic to paramagnetic dissipative phase transition. This approximation

neglects nonlocal quantum correlations while capturing the on-site correlations and classical spatial (nonlocal) correlations. Furthermore, this approach introduces a reduced Hilbert space that scales linearly with system size, allowing for the simulation of relatively large lattices. By considering individual trajectories, we identify features of the different phases, and for finite lattices sizes we find an intermediate regime where both phases are metastable and the dynamics exhibit switching between them. The transition is also explored by calculating the spin structure (SS) factor which is qualitatively in agreement with the earlier results of Ref. [28]. We also examine the spatial dependence of the correlation function which in the paramagnetic phase reveals remnants of a long-range antiferromagnetic order. Our results show that it is sufficient to consider the nonlocal classical fluctuations to at least qualitatively capture parts of the phase diagram that are not identified by standard Gutzwiller mean-field theories.

The paper is organized as follows: In the second section we introduce the dissipative XYZ model, the third section discusses the Gutzwiller Monte Carlo approach, and in the fourth section the results of the simulations are presented. Finally, in the last section, the conclusions and perspectives are presented.

II. THE DISSIPATIVE XYZ MODEL

The anisotropic XYZ-Heisenberg Hamiltonian is given by (in units with $\hbar = 1$),

$$\hat{H} = \sum_{\langle \mathbf{i}, \mathbf{j} \rangle} \left(J_x \hat{\sigma}_{\mathbf{i}}^{(x)} \hat{\sigma}_{\mathbf{j}}^{(x)} + J_y \hat{\sigma}_{\mathbf{i}}^{(y)} \hat{\sigma}_{\mathbf{j}}^{(y)} + J_z \hat{\sigma}_{\mathbf{i}}^{(z)} \hat{\sigma}_{\mathbf{j}}^{(z)} \right), \quad (1)$$

where $\sigma_{\mathbf{i}}^{(\alpha)}$ are the Pauli matrices (with $\alpha = \{x,y,z\}$) for spin $\mathbf{i}$ and the sum is over all nearest neighbors. The parameters J_x, J_y, and J_z are the coupling strengths for the x, y, and z spin components, respectively. The Hamiltonian (1) determines the unitary part of the time evolution. The full time evolution of the dissipative XYZ model, including the dissipation along the z direction, is described by a Lindblad-master equation for the

density-matrix $\hat{\rho}$,

$$\partial_t \hat{\rho} = -i[\hat{H}, \hat{\rho}] + \frac{\gamma}{2} \sum_{\mathbf{j}} (2\hat{\sigma}_{\mathbf{j}}^{(-)} \hat{\rho} \hat{\sigma}_{\mathbf{j}}^{(+)} - \{\hat{\sigma}_{\mathbf{j}}^{(+)} \hat{\sigma}_{\mathbf{j}}^{(-)}, \hat{\rho}\}), \quad (2)$$

where γ is the decay rate of the spins and $\sigma_i^{(\pm)}$'s are the raising $(+)$ and lowering $(-)$ operators along the z axis. The master equation (2) has a $\mathbb{Z}_2$ symmetry: $(\hat{\sigma}_n^{(x)}, \hat{\sigma}_n^{(y)}) \rightarrow (-\hat{\sigma}_n^{(x)}, -\hat{\sigma}_n^{(y)})$. This symmetry can be spontaneously broken in an ordered phase, such as a ferromagnet with a finite magnetization on the xy plane [27,28].

The dissipative XYZ model has been studied by various methods. In Ref. [27] a single-site mean-field calculation revealed that the competition between precessional and dissipative dynamics leads to a very rich phase diagram. In Ref. [28] more advanced numerical approaches were applied to a particular region of the phase diagram containing a paramagnetic to ferromagnetic phase transition. Using a matrix product operator ansatz for the density matrix they revealed the absence of a phase transition in one dimension. For two dimensions they included the nonlocal correlations on a relatively short range with the cluster mean-field approach. This revealed that, although the single-site mean-field approach predicts a ferromagnetic phase all the way to $J_y \rightarrow \infty$, the cluster mean-field approach predicts a paramagnetic phase for large J_y. For the parameter values of $J_x = 0.9\gamma$ and $J_z = \gamma$ a finite-size scaling revealed that in the thermodynamic limit the system exhibits a ferromagnetic phase for $1.04\gamma \lesssim J_y \lesssim 1.4\gamma$ [28]. We will consider the same parameter range.

III. THE GUTZWILLER MONTE CARLO APPROACH

The Gutzwiller Monte Carlo approach is a combination of the Gutzwiller ansatz for the wave function and the wave-function Monte Carlo simulation. We start by briefly discussing these two methods.

The Gutzwiller ansatz Ψ_{GW} corresponds to a product wave function [30],

$$\Psi_{GW}(\{i\}) = \prod_i \psi_i, \quad (3)$$

where the index i denotes the different modes or lattice sites and ψ_i is a single-mode wave function on site i. This ansatz neglects the spatial correlations whereas the local correlations are fully taken into account. The dimension of the wave-function Ψ_{GW} grows linearly with the system size N as Nd with d as the local Hilbert space dimension rather than the exponential increase d^N for the full wave function. A well-known application of the Gutzwiller wave-function (3) is for the description of a superfluid to Mott insulator transition [31,32]. More recently, the Gutzwiller ansatz has been extended for the description of dissipative lattice systems by decoupling the full density matrix as a direct product of single-site density matrices (see, for example, Refs. [18,27,28,33–36]).

The wave-function Monte Carlo (also known as quantum trajectories) is a simulation technique for dissipative systems which keeps track of the wave function during individual realizations [37–39]. The evolution of the wave function is determined by stochastically simulating an external measurement of the excitations that leave the system. This corresponds

to an exact simulation technique, and the full density matrix can be obtained by averaging over the individual realizations.

If one is interested in describing systems containing multiple coupled modes, such as a lattice model, one quickly runs into a prohibitively large Hilbert space which grows exponentially with the system size. The Gutzwiller Monte Carlo approach deals with this by combining the relative small effective Hilbert space of the Gutzwiller ansatz (3) with the wave-function Monte Carlo. In practice, a wave-function Monte Carlo simulation is performed while restricting the wave function to the subspace of product wave functions (3) (see the Appendix for more technical details). This captures all the local correlations whereas nonlocal quantum correlations are neglected. This can be understood by considering a general two-point correlation function (with $\mathbf{i} \neq \mathbf{j}$),

$$\langle \hat{\sigma}_{\mathbf{i}}^{(\alpha)} \hat{\sigma}_{\mathbf{j}}^{(\beta)} \rangle = \frac{1}{T} \sum_t^T \langle \Psi_{GW}^{(t)}(\{\mathbf{i}\}) | \hat{\sigma}_{\mathbf{i}}^{(\alpha)} \hat{\sigma}_{\mathbf{j}}^{(\beta)} | \Psi_{GW}^{(t)}(\{\mathbf{i}\}) \rangle$$

$$= \frac{1}{T} \sum_t^T \langle \psi_{\mathbf{i}}^{(t)} | \hat{\sigma}_{\mathbf{i}}^{(\alpha)} | \psi_{\mathbf{i}}^{(t)} \rangle \langle \psi_{\mathbf{j}}^{(t)} | \hat{\sigma}_{\mathbf{j}}^{(\beta)} | \psi_{\mathbf{j}}^{(t)} \rangle, \quad (4)$$

where the index t denotes the different trajectories and T is the total number of trajectories. This shows that there are no spatial correlations within a single trajectory since all expectation values with respect to the Gutzwiller wave function decouple. Importantly, nonlocal classical correlations are included by averaging over the different realizations. These are neglected with a Gutzwiller decoupling of the density matrix. Recently this approach was applied for the description of the optically bistable driven-dissipative Bose-Hubbard dimer [40].

The validity of the method is determined by the role of the nonlocal quantum correlations and whether classical correlations are sufficient to describe the system. This argument could be reversed by noting that if the Gutzwiller Monte Carlo approach succeeds in capturing the behavior of the system nonlocal quantum correlations are not important. An interesting question is then to which extent the critical behavior of dissipative systems is captured. This is also motivated by recent works that show that some critical dissipative quantum models can be mapped onto a classical system [41,42]. With this in mind we explore the properties of the critical dissipative XYZ model with the Gutzwiller Monte Carlo approach.

IV. RESULTS

For the simulations we consider finite 2D symmetric lattices of various sizes with periodic boundary conditions and total number of lattice sites N [43]. We always use the system parameters $J_x = 0.9\gamma$ and $J_z = \gamma$ and vary J_y. For these parameters the single-site mean-field approach predicts a transition from a paramagnetic to a ferromagnetic phase at $J_y \approx 1.04\gamma$ [27]. The more advanced cluster mean-field approach revealed another ferromagnetic to paramagnetic phase transition at $J_y \approx 1.4\gamma$ in the thermodynamic limit [28].

Care has to be taken when choosing the initial state for the Gutzwiller Monte Carlo simulations. A possible issue arises when the system reaches the pure state with all spins pointing downwards in the z direction. This is the exact steady state of the dissipative XXZ model, corresponding to $J_x = J_y$ [27].

However, within the considered Gutzwiller approximation, it becomes an artificial dark state for all possible system parameters since it is not possible to reach a finite magnetization on the xy plane starting from zero. The same behavior is encountered with the single-site mean-field approach [27]. This is clearly an artifact of the approximation since the unitary evolution in the full Hilbert space, determined by the XYZ-Hamiltonian (1), can lead to fluctuations of the magnetization on the xy plane starting from zero (this can easily be verified by just considering two coupled spins). Because of this the initial state should have a finite magnetization on the xy plane and in practice we always consider an initial state with all spins aligned with the x direction.

We start by considering the magnetization M_x in the x direction,

$$M_x = N^{-1} \sum_{\mathbf{i}} \langle \hat{\sigma}_{\mathbf{i}}^{(x)} \rangle. \tag{5}$$

This quantity is presented in Fig. 1 for a 6×6 lattice as a function of time during single trajectories. The different panels correspond to different values of J_y. For (a) $J_y = \gamma$ the system relaxes to a pure steady state with all spins pointing downward in the z direction and $M_x = 0$ as also predicted by the single-site mean-field approach [27]. As the system gets trapped in this artificial dark state (see the discussion above) the fluctuations around this state, as observed in Refs. [28,29], are not captured. For (b) $J_y = 1.2\gamma$ the system exhibits a ferromagnetic phase with on average a nonzero magnetization. Depending on whether the initial spins are aligned with the positive $(+)$ or negative $(-)$ x direction M_x stays positive or negative, respectively. For (c) the value of $J_y = 1.8\gamma$ the system switches on a relatively long time scale between the two ferromagnetic phases which are stable for smaller values of J_y and a paramagnetic phase which becomes stable at larger J_y. This paramagnetic phase is clearly visible for (d) $J_y = 2.5\gamma$ with a magnetization which fluctuates around zero.

To further explore the different phases in the steady state we now consider the steady-state spin structure factor $S_{\mathrm{SS}}^{xx}(\mathbf{k} = \mathbf{0})$, where

$$S_{\mathrm{SS}}^{xx}(\mathbf{k}) = \frac{1}{N(N-1)} \sum_{\mathbf{j} \neq \mathbf{l}} e^{-i\mathbf{k} \cdot (\mathbf{j} - \mathbf{l})} \langle \hat{\sigma}_{\mathbf{j}}^{(x)} \hat{\sigma}_{\mathbf{l}}^{(x)} \rangle. \tag{6}$$

A nonzero value of $S_{\mathrm{SS}}^{xx}(\mathbf{0})$ indicates the presence of a ferromagnetic phase, and it is zero in the paramagnetic phase. In Fig. 2 $S_{\mathrm{SS}}^{xx}(\mathbf{0})$ is presented as a function of J_y for different lattice sizes. The steady-state results are obtained by averaging a single trajectory over a total time of $10\,000/\gamma$ and $40\,000/\gamma$ in the intermediate regime for the two largest lattices. The result from the single-site MF approach is also presented which predicts a ferromagnetic phase for $J_y \gtrsim 1.04\gamma$ with

$$S_{\mathrm{SS}}^{xx}(\mathbf{0}) = M_x^{(\mathrm{MF})} M_x^{(\mathrm{MF})}$$

$$= \frac{\gamma}{8} \left(\frac{\gamma}{16} \sqrt{\frac{1}{(J_z - J_x)(J_y - J_z)}} - 1 \right)$$

$$\times \sqrt{\frac{1}{(J_z - J_x)(J_y - J_z)}} \frac{J_y - J_z}{J_x - J_y}, \tag{7}$$
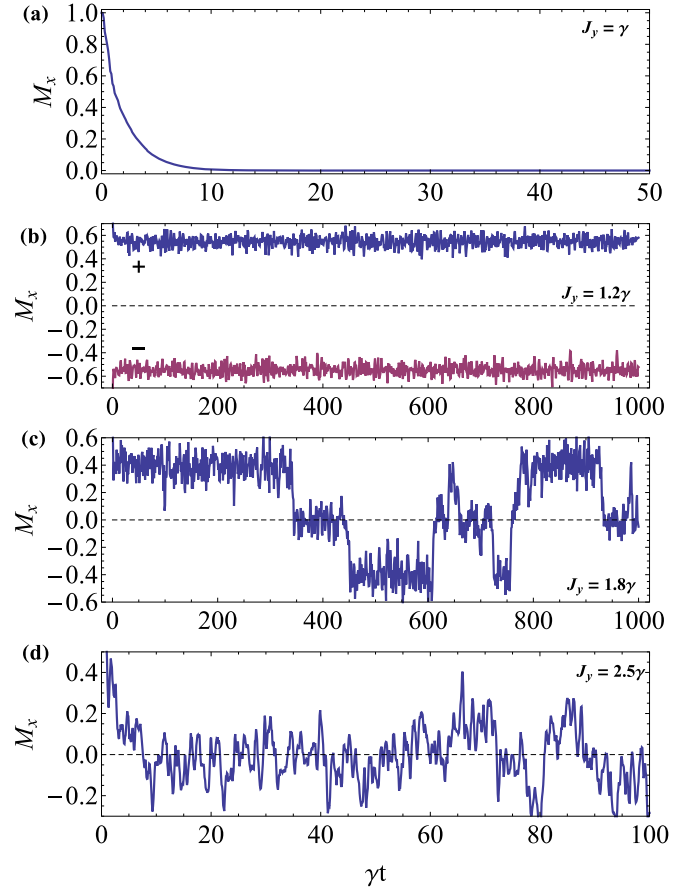

FIG. 1. The magnetization in the x direction (5) as a function of time on a 6×6 lattice during individual trajectories for four representative values of J_y: (a) γ, (b) 1.2γ, (c) 1.8γ, and (d) 2.5γ. Initially all spins are aligned parallel with the x axis in the positive direction [except for the second panel with $J_y = 1.2$ where results are shown with initial spins both in the positive $(+)$ and in the negative $(-)$ x directions]. The different phases are clearly visible: A paramagnetic phase with $M_x = 0$ for $J_y = \gamma$, a ferromagnetic phase with $M_x \neq 0$ for $J_y = 1.2\gamma$, and another paramagnetic phase for $J_y = 2.5\gamma$ with $M_x = 0$ on average. For $J_y = 1.8\gamma$ the system exhibits an intermediate regime where the system switches between the different phases on a relatively large time scale (note the different scales for the time).

where $M_x^{(\mathrm{MF})}$ is the single-site mean-field result for the magnetization in the x direction [27,28]. Close to the transition at $J_y \approx 1.04$ the results for finite lattice sizes in Fig. 2 are in good agreement with the single-site mean-field result (7) which is also predicted by the cluster mean-field approach [28]. For values of J_y just above this transition the results converge to a finite value as a function of the lattice size, revealing the presence of a ferromagnetic phase in the thermodynamic limit. For large values of J_y the spin structure factor $S_{\mathrm{SS}}^{xx}(\mathbf{0})$ decreases to zero as the lattice size is increased, indicating a paramagnetic phase in the thermodynamic limit. These results show the presence of a ferromagnetic to paramagnetic transition in the thermodynamic limit which is not captured by the single-site mean-field result (7) as also predicted by the cluster mean-field approach [28]. As the system size is increased the ferromagnetic region shrinks and the transition
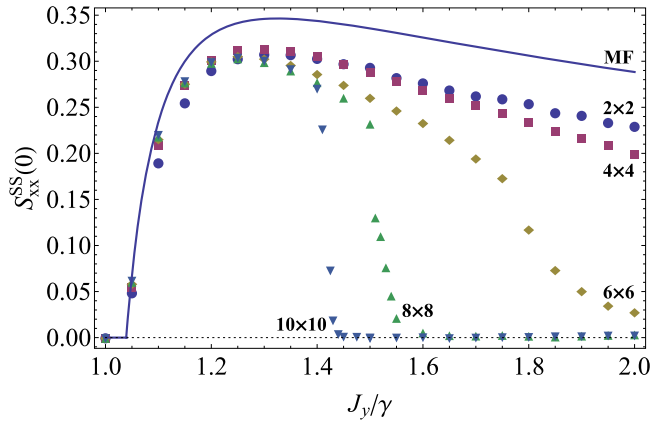
FIG. 2. The spin structure factor $S_{xx}^{SS}(0)$ (6) for finite two-dimensional lattices as a function of the coupling J_y (in units of γ). The full line is the single-site MF result (7) which predicts a nonzero value for $J_y \gtrsim 1.04\gamma$, corresponding to a ferromagnetic phase. The markers are the results from the Gutzwiller Monte Carlo approach obtained by averaging a single trajectory over a total time of $10\,000/\gamma$ for various system sizes (as indicated in the figure) and $40\,000/\gamma$ in the intermediate regime for the two largest lattices. This reveals a transition to a paramagnetic phase with $S_{SS}^{xx}(0) = 0$ for large J_y which as the system size is increased becomes sharper with a shrinking ferromagnetic region.

FIG. 3. The correlation function $\langle \hat{\sigma}_{\mathbf{i}}^{(x)} \hat{\sigma}_{\mathbf{j}}^{(x)} \rangle$ as a function of the distance $r = |\mathbf{i} - \mathbf{j}|$ for a 12×12 lattice and for $J_y = 1.2\gamma$ (circles), 1.7γ (squares), and 2γ (triangles). The results are obtained with the Gutzwiller Monte Carlo approach by averaging a single trajectory over a total time of $20\,000/\gamma$. For $J_y = 1.2\gamma$ the correlation function converges to a finite value as expected in the ferromagnetic phase. For $J_y = 1.7\gamma$ the correlation function decays and becomes negative at relatively long distances, corresponding to a long-scale antiferromagnetic ordering. For longer distances the correlation function is expected to eventually decay to zero as observed for $J_y = 2\gamma$. The smaller symbols are the result from the cluster mean-field approach for $J_y = 1.2\gamma$ and 1.7γ [28]. The inset shows the correlation function as a function of the distance in the x and y directions for $J_y = 1.7\gamma$.

becomes sharper which indicates that in the thermodynamic limit the intermediate regime where both phases are metastable (see the third panel of Fig. 1) disappears. The observed behavior is in qualitative agreement with the results of the cluster mean-field approach which predicts a ferromagnetic phase for $1.04\gamma \lesssim J_y \lesssim 1.4\gamma$ in the thermodynamic limit [28].

In Fig. 3 the average steady-state correlation function $\langle \hat{\sigma}_{\mathbf{i}}^{(x)} \hat{\sigma}_{\mathbf{j}}^{(x)} \rangle$ is presented for a 12×12 lattice as a function of the Euclidian distance $r = |\mathbf{i} - \mathbf{j}|$. For $J_y = 1.2\gamma$ the correlation function converges to a nonzero value for long distances as expected for the ferromagnetic phase. For $J_y = 1.7\gamma$ the correlation function decays and becomes negative at relatively long distances, revealing remnants of antiferromagnetic ordering at a relatively long scale. For longer distances the correlation function is expected to decay towards zero as observed for $J_y = 2\gamma$ and as expected for the paramagnetic phase. As a consequence of the periodic boundary conditions not all the points in Fig. 3 are on a smooth curve. To clarify this, the correlation function is also plotted as a function of the distance in the x and in the y directions in the inset of Fig. 3. Along a lattice direction the boundary is reached at a shorter distance with respect to a diagonal direction. For larger lattices this effect should become weaker, and in the thermodynamic limit the points are expected to converge to a smooth curve. The results from the cluster mean-field approach for a 4×4 cluster of Ref. [28] are also presented in Fig. 3 for $J_y = 1.2\gamma$ and 1.7γ (smaller symbols). For $J_y = 1.2\gamma$ these results qualitatively agree, but our correlation is a bit stronger. For $J_y = 1.7\gamma$ the correlation function obtained in Ref. [28] initially increases and then weakly decreases which is different from the Gutzwiller Monte Carlo prediction which exhibits a monotonous decaying behavior at this length scale. The length scale considered with the cluster mean-field approach is too
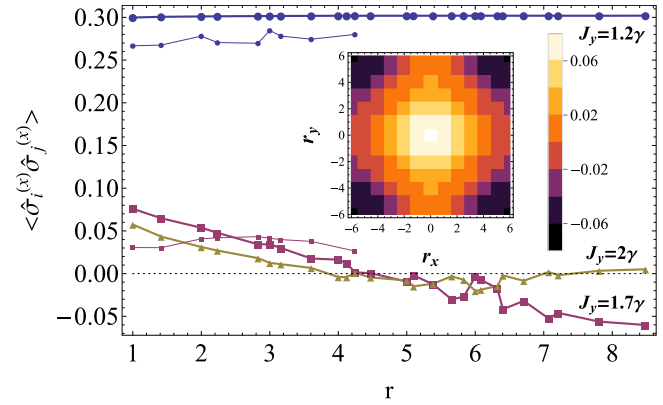
small to compare the long-range antiferromagnetic behavior. It is not clear whether these deviations are due to the relatively small size of the considered cluster in Ref. [28] or due to the Gutzwiller approximation. It would be interesting to compare the results with other numerical approaches that capture all correlations, such as the corner-space renormalization method [22,29].

It is clear that the two paramagnetic phases are actually very different in nature. For small values of J_y ($J_y \lesssim 1.04\gamma$) all spins point downward in the z direction whereas for large values of J_y the spins fluctuate around zero magnetization in the x direction (see Fig. 1). This shows that in the latter paramagnetic phase the entropy is much higher. This has been suggested as the driving mechanism behind the reentrance of a paramagnetic phase which is not captured at the mean-field level [28].

V. CONCLUSIONS AND PERSPECTIVES

We considered the Gutzwiller Monte Carlo approach for the description of the critical dissipative XYZ model which allows to efficiently simulate relatively large lattice sizes. This corresponds to neglecting the nonlocal quantum correlations whereas capturing the classical spatial correlations. Our results reveal the presence of a transition from a ferromagnetic to paramagnetic phase which is not captured by the single-site mean-field treatment presented in Ref. [27]. This behavior is at least qualitatively in agreement with earlier work that includes short-range correlations in Ref. [28]. A comparison of the spatial correlation function on the other hand revealed deviations with the results of Ref. [28]. This reveals the potential of the Gutzwiller Monte Carlo approach to become

an important tool for the description of dissipative phase transitions.

The approach can be straightforwardly generalized to other dissipative lattice systems, such as the driven-dissipative Bose-Hubbard model [44] and a lattice of coupled Jaynes-Cummings resonators [13]. This could shed new light on the role of quantum correlations for dissipative phase transitions. Also dynamical properties of critical systems could be explored by the Gutzwiller Monte Carlo approach. This gives access to the Liouvillian gap which has been shown to be an important property for the characterization of dissipative phase transitions [4,8,13,16,35].

In the same spirit as the Gutzwiller Monte Carlo approach one could use other variational wave functions in combination with a wave function Monte Carlo simulation. A straightforward extension would be to include short-range quantum correlations in the wave function. This could be performed by considering a sublattice of clusters and keeping track of all (quantum and classical) correlations within the clusters whereas only classical correlations are considered between them. For the considered dissipative XYZ model this could solve the issue with the artificial dark state at small J_y already by considering a sublattice of clusters of size 2×1. It would also be interesting to examine how this affects the critical exponents and whether it could lead to beyond mean-field predictions.

Another perspective is to add an external probe to the Hamiltonian and examine the susceptibility. This approach was followed with the corner-space renormalization method in Ref. [29].

APPENDIX: DETAILS OF THE GUTZWILLER MONTE CARLO APPROACH

Between the jumps the time evolution of the wave function is determined by the following effective mean-field Hamiltonian (which is non-Hermitian and nonlinear):

$$\hat{H} = \sum_{\mathbf{i}} \left(J_x \hat{\sigma}_{\mathbf{i}}^{(x)} \sum_{\langle \mathbf{j} \rangle} \langle \hat{\sigma}_{\mathbf{j}}^{(x)} \rangle + J_y \hat{\sigma}_{\mathbf{i}}^{(y)} \sum_{\langle \mathbf{j} \rangle} \langle \hat{\sigma}_{\mathbf{j}}^{(y)} \rangle \right.$$
$$\left. + J_z \hat{\sigma}_{\mathbf{i}}^{(z)} \sum_{\langle \mathbf{j} \rangle} \langle \hat{\sigma}_{\mathbf{j}}^{(z)} \rangle - i \frac{\gamma}{2} \hat{\sigma}_{\mathbf{i}}^{(+)} \hat{\sigma}_{\mathbf{i}}^{(-)} \right), \quad \text{(A1)}$$

where we used the notation $\sum_{\langle \mathbf{j} \rangle}$ to indicate a summation over all sites $\mathbf{j}$ that are nearest neighbors of site $\mathbf{i}$. We also introduced the expectation values,

$$\langle \hat{\sigma}_{\mathbf{j}}^{(\alpha)} \rangle = \langle \Psi_{GW}(\{\mathbf{i}\}) | \hat{\sigma}_{\mathbf{j}}^{(\alpha)} | \Psi_{GW}(\{\mathbf{i}\}) \rangle$$
$$= \langle \psi_{\mathbf{j}} | \hat{\sigma}_{\mathbf{j}}^{(\alpha)} | \psi_{\mathbf{j}} \rangle. \quad \text{(A2)}$$

Since the Hamiltonian (A1) is non-Hermitian the norm of the wave function decays as a function of time. When the norm decays below a randomly determined value a jump is performed in the simulation. The site $\mathbf{i}$ on which the jump occurs is chosen according to the probability distribution $P_{\mathbf{i}}$,

$$P_{\mathbf{i}} = \frac{\langle \psi_{\mathbf{i}} | \hat{\sigma}^{(+)} \hat{\sigma}_{\mathbf{i}}^{(-)} | \psi_{\mathbf{i}} \rangle}{\langle \psi_{\mathbf{i}} | \psi_{\mathbf{i}} \rangle}. \quad \text{(A3)}$$

A jump on a site i corresponds to setting the spin downward in the z direction. After the jump the wave function is normalized and then further evolved according to the effective Hamiltonian (A1) until the norm drops again below a (new) randomly determined value. This procedure is repeated until the desired total time is reached.

[1] I. Carusotto and C. Ciuti, Rev. Mod. Phys. **85**, 299 (2013).

[2] C. Noh and D. G. Angelakis, Rep. Prog. Phys. **80**, 016401 (2017).

[3] M. J. Hartmann, J. Opt. **18**, 104005 (2016).

[4] E. M. Kessler, G. Giedke, A. Imamoglu, S. F. Yelin, M. D. Lukin, and J. I. Cirac, Phys. Rev. A **86**, 012116 (2012).

[5] H. J. Carmichael, Phys. Rev. X **5**, 031028 (2015).

[6] W. Casteels, F. Storme, A. Le Boité, and C. Ciuti, Phys. Rev. A **93**, 033824 (2016).

[7] J. J. Mendoza-Arenas, S. R. Clark, S. Felicetti, G. Romero, E. Solano, D. G. Angelakis, and D. Jaksch, Phys. Rev. A **93**, 023821 (2016).

[8] W. Casteels, R. Fazio, and C. Ciuti, Phys. Rev. A **95**, 012128 (2017).

[9] N. Bartolo, F. Minganti, W. Casteels, and C. Ciuti, Phys. Rev. A **94**, 033841 (2016).

[10] V. Savona, Phys. Rev. A **96**, 033826 (2017).

[11] E. Mascarenhas, G. Giudice, and V. Savona, Quantum **1**, 40 (2017).

[12] P. Hamel, S. Haddadi, F. Raineri, P. Monnier, G. Beaudoin, I. Sagnes, A. Levenson, and A. M. Yacomotti, Nat. Photonics **9**, 311 (2015).

[13] M. Fitzpatrick, N. M. Sundaresan, A. C. Y. Li, J. Koch, and A. A. Houck, Phys. Rev. X **7**, 011016 (2017).

[14] J. M. Fink, A. Dombi, A. Vukics, A. Wallraff, and P. Domokos, Phys. Rev. X **7**, 011012 (2017).

[15] S. R. K. Rodriguez, W. Casteels, F. Storme, N. Carlon Zambon, I. Sagnes, L. Le Gratiet, E. Galopin, A. Lemaître, A. Amo, C. Ciuti, and J. Bloch, Phys. Rev. Lett. **118**, 247402 (2017).

[16] T. Fink, A. Schade, S. Höfling, C. Schneider, and A. İmamoğlu, Nat. Phys. **14**, 365 (2018).

[17] R. Orús and G. Vidal, Phys. Rev. B **78**, 155117 (2008).

[18] A. Le Boité, G. Orso, and C. Ciuti, Phys. Rev. Lett. **110**, 233601 (2013).

[19] P. Degenfeld-Schonburg and M. J. Hartmann, Phys. Rev. B **89**, 245108 (2014).

[20] J. Cui, J. I. Cirac, and M. C. Bañuls, Phys. Rev. Lett. **114**, 220601 (2015).

[21] E. Mascarenhas, H. Flayac, and V. Savona, Phys. Rev. A **92**, 022116 (2015).

[22] S. Finazzi, A. Le Boité, F. Storme, A. Baksic, and C. Ciuti, Phys. Rev. Lett. **115**, 080604 (2015).

[23] A. C. Y. Li, F. Petruccione, and J. Koch, Phys. Rev. X **6**, 021037 (2016).

[24] W. Casteels, S. Finazzi, A. L. Boité, F. Storme, and C. Ciuti, New J. Phys. **18**, 093007 (2016).

[25] A. Kshetrimayum, H. Weimer, and R. Orús, Nat. Commun. **8**, 1291 (2017).

[26] A. Biella, J. Jin, O. Viyuela, C. Ciuti, R. Fazio, and D. Rossini, Phys. Rev. B **97**, 035103 (2018).

[27] T. E. Lee, S. Gopalakrishnan, and M. D. Lukin, Phys. Rev. Lett. **110**, 257204 (2013).

[28] J. Jin, A. Biella, O. Viyuela, L. Mazza, J. Keeling, R. Fazio, and D. Rossini, Phys. Rev. X **6**, 031011 (2016).

[29] R. Rota, F. Storme, N. Bartolo, R. Fazio, and C. Ciuti, Phys. Rev. B **95**, 134431 (2017).

[30] M. C. Gutzwiller, Phys. Rev. Lett. **10**, 159 (1963).

[31] D. S. Rokhsar and B. G. Kotliar, Phys. Rev. B **44**, 10328 (1991).

[32] W. Krauth, M. Caffarel, and J.-P. Bouchaud, Phys. Rev. B **45**, 3137 (1992).

[33] S. Diehl, A. Tomadin, A. Micheli, R. Fazio, and P. Zoller, Phys. Rev. Lett. **105**, 015702 (2010).

[34] J. Jin, D. Rossini, M. Leib, M. J. Hartmann, and R. Fazio, Phys. Rev. A **90**, 023827 (2014).

[35] R. M. Wilson, K. W. Mahmud, A. Hu, A. V. Gorshkov, M. Hafezi, and M. Foss-Feig, Phys. Rev. A **94**, 033801 (2016).

[36] M. Biondi, G. Blatter, H. E. Türeci, and S. Schmidt, Phys. Rev. A **96**, 043809 (2017).

[37] J. Dalibard, Y. Castin, and K. Mølmer, Phys. Rev. Lett. **68**, 580 (1992).

[38] K. Mølmer, Y. Castin, and J. Dalibard, J. Opt. Soc. Am. B **10**, 524 (1993).

[39] H. J. Carmichael, Phys. Rev. Lett. **70**, 2273 (1993).

[40] W. Casteels and M. Wouters, Phys. Rev. A **95**, 043833 (2017).

[41] M. F. Maghrebi and A. V. Gorshkov, Phys. Rev. B **93**, 014307 (2016).

[42] M. Foss-Feig, P. Niroula, J. T. Young, M. Hafezi, A. V. Gorshkov, R. M. Wilson, and M. F. Maghrebi, Phys. Rev. A **95**, 043826 (2017).

[43] We have simulated spin lattices with sizes of up to 12×12 sites. For the description of a quantum system this corresponds to an enormous Hilbert space, and this is possible only thanks to neglecting nonlocal quantum effects. For the description of a classical system this is however not very large, and we have limited the system size in order to obtain good convergence of the results in a manageable time. We note that the simulations were not fully optimized, and it should be possible to reach much larger system sizes by, for example, parallelizing the algorithm.

[44] A. Amo and J. Bloch, C. R. Phys. **17**, 934 (2016).